Spectral diffusion in glasses under high pressure: A study by time-resolved hole-burning

A. J. Lock, T. M. H. Creemers, and S. Völker[a)]
Center for the Study of Excited States of Molecules, Huygens and Gorlaeus Laboratories, University of Leiden, P.O. Box 9504, 2300 RA Leiden, The Netherlands

(Received 30 November 1998; accepted 22 January 1999)

We have studied optical dephasing and spectral diffusion of the $S_1 \leftarrow S_0$ 0–0 transition of bacteriochlorophyll-*a* (BChl-*a*) in the glass 2-methyltetrahydrofuran (MTHF) at ambient ($\Delta p = 0$) and high pressure ($\Delta p = 3.6$ GPa) between 1.2 and 4.2 K by time-resolved hole-burning. The ''effective'' homogeneous linewidth Γ'_{hom} follows a power law dependence on temperature, $\Gamma'_{\mathrm{hom}} = \Gamma'_0 + aT^{1.3\pm0.1}$, where $\Gamma'_0 = \Gamma_0 + \Gamma_0^{\mathrm{ET}} + \Gamma_0^{\mathrm{ET}\rightarrow\mathrm{SD}}(t_d)$ is the residual linewidth and $a = a_{\mathrm{PD}} + a_{\mathrm{SD}}(t_d) + a_{\mathrm{ET}\rightarrow\mathrm{SD}}(t_d)$ is the coupling constant. The separate contributions to Γ'_0 and a are the fluorescence decay rate $\Gamma_0 = (2\pi\tau_{\mathrm{fl}})^{-1}$, the ''downhill'' energy-transfer rate Γ_0^{ET}, the coupling constants due to ''pure'' dephasing a_{PD} and ''normal'' spectral diffusion $a_{\mathrm{SD}}(t_d)$, and two terms related to ''extra'' spectral diffusion induced by energy transfer, $\Gamma_0^{\mathrm{ET}\rightarrow\mathrm{SD}}(t_d)$ and $a_{\mathrm{ET}\rightarrow\mathrm{SD}}(t_d)$. We have quantitatively analyzed these contributions at ambient and high pressure. The results show that ''normal'' SD, ''extra'' SD, and ET→SD are strongly influenced by pressure. We have interpreted our findings in terms of a change in the number of two-level-systems, the low-frequency modes characteristic for the glassy state. © *1999 American Institute of Physics.* [S0021-9606(99)70415-0]

I. INTRODUCTION

Spectral diffusion (SD), or the increase of the ''effective'' homogeneous linewidth Γ'_{hom} of a chromophore doped in a glass at low temperature, arises from frequency fluctuations of the optical transition of the probe molecule caused by structural relaxation of the host.[1–6] A glass is assumed to consist of low-energy excitations called two-level systems (TLSs). These are double-well potentials representing distinct structural configurations of the glass.[7,8] A change in the structure is described as a transition or ''flipping'' from one potential well to another due to interaction with phonons. TLSs are assumed to have a broad distribution of tunneling parameters and energy splittings, leading to a broad distribution of fluctuation rates.[9–11] As a consequence, and due to the coupling between the probe molecule and the glass, Γ'_{hom} increases with experimental delay time over many orders of magnitude in time.[2,5,6] If TLSs were associated with voids or excess free volume in the glass, as proposed in the literature,[12] one would expect that the number (or density) of TLSs and, therefore, the amount of spectral diffusion would decrease under high pressure. We will show that such a picture is in agreement with the experimental results here presented.

In doped organic glasses at low temperatures ($T \leqslant 10$ K) and low concentrations ($c \leqslant 5\times10^{-4}$ M), Γ'_{hom} obeys a $T^{1.3}$ power law,[6,13–17] independent of the glass and the probe:

$$\Gamma'_{\mathrm{hom}} = \Gamma_0 + [a_{\mathrm{PD}} + a_{\mathrm{SD}}(t_d)]T^{1.3\pm0.1}, \tag{1.1}$$

where $\Gamma_0 = (2\pi\tau_{\mathrm{fl}})^{-1}$ is determined by the intrinsic fluorescence lifetime τ_{fl} of the probe molecule, a_{PD} is the ''pure'' dephasing coupling constant, and $a_{\mathrm{SD}}(t_d)$ is the coupling constant due to normal spectral diffusion, with t_d the delay time between excitation and probing.[6] The observed $T^{1.3}$ power law has been explained with the standard TLS model[7,8] by assuming a dipole–dipole coupling between the probe molecule and the TLSs, with a density of states of the TLSs varying as $\rho \propto E^{0.3}$, where E is the energy splitting of the eigenstates of the TLSs.[3,4,18,19] Recently, Silbey *et al.*[6] explained the intertwined dependence of T and t_d by assuming a slight modification of the standard model.[7,8]

At higher concentrations, downhill energy transfer (ET) between probe molecules may take place. This leads to a shortening of the excited-state lifetime and an increase of Γ'_{hom} through the residual linewidth. The latter is then equal to $\Gamma'_0 = \Gamma_0 + \Gamma_0^{\mathrm{ET}}$, where Γ_0^{ET} is the energy-transfer rate. In addition to this process, a remarkable new effect was recently discovered in our group: energy-transfer-induced spectral diffusion (ET→SD).[20–23] This effect depends on concentration c, excitation wavelength λ_{exc} and delay time t_d. It contributes to the residual linewidth Γ'_0 and to the coupling constant a in the temperature-dependent term of Γ'_{hom} in Eq. (1.1) with an extra term.

In a previous study, where hole-burning was combined with high pressure ($\Delta p = 3.4$ GPa),[21] we have found that the temperature dependence of Γ'_{hom} of bacteriochlorophyll-*a* (BChl-*a*) doped in triethylamine (TEA) changed from a $T^{1.3\pm0.1}$ power law, typical for glassy systems, to an exponential dependence on T, $\exp(-E/kT)$, characteristic for crystalline materials. We concluded from these results that local order had been induced in TEA under high pressure.[21] Crystallization effects have also been observed with other tech-

[a)]Author to whom correspondence should be addressed.

niques in methanol[24] and ethanol[25] at room temperature at pressures between 5 and 10.5 GPa, and 1.8 GPa, respectively.

In this work we were interested in the effect of high pressure on a ''true'' glass, i.e., a system that remains glassy at pressures up to 3–4 GPa. In particular, we wanted to investigate, in a quantitative manner, the relation between pressure and the amount of spectral diffusion in the absence and presence of downhill energy transfer (ET). Furthermore, we wanted to test whether TLSs are representative of the free volume in the glass. We chose for these experiments the system BChl-*a* in 2-methyltetrahydrofuran (MTHF) at a concentration $c \sim 5\times10^{-4}$ M. MTHF forms a ''true'' glass and shows downhill ET at this concentration. Our hole-burning experiments at high pressure ($\Delta p = 3.6$ GPa), carried out as a function of temperature ($T = 1.2-4.2$ K), excitation wavelength (λ_{exc} in the blue and red wings of the $S_1 \leftarrow S_0$ 0–0 band), and delay time ($t_d = 10^{-5}-10^{5}$ s) are compared to those obtained at ambient pressure ($\Delta p = 0$).

In Sec. II, we describe the sample preparation and the calibration of the pressure in the cell at liquid-He temperatures, the experimental setup for time-resolved hole-burning and the determination of Γ'_{hom} from the hole width. In Sec. III, results are presented on optical dephasing, energy transfer, ''normal,'' and ''extra'' spectral diffusion over ten orders of magnitude in time. These results are then discussed quantitatively in terms of our newly discovered ET→SD process.[22,23] The interpretation of the results is summarized in Sec. IV where the role played by TLSs in glasses under high pressure is highlighted.

II. EXPERIMENT

A. Sample preparation and pressure cell

BChl-*a* was extracted from purple bacteria *Rhodobacter sphaeroides* and isolated following a slightly modified version[21,26] of the method of Iriyama *et al.*[27] BChl-*a* was dissolved in ether to an optical density OD=1/mm at 770 nm and stored at −20 °C. Samples of BChl-*a* in 2-methyltetrahydrofuran (MTHF) were prepared by evaporating the ether from BChl-*a* and then dissolving the remaining film in MTHF. The samples had a concentration $c \sim 5\times10^{-4}$ M. The optical density in the pressure cell was OD∼0.5 at the maximum of the absorption band.

For the high-pressure experiments we have used a diamond-anvil cell of the Merrill–Bassett type,[28,29] as previously described.[21] The pressure was calibrated by means of a small ruby splinter introduced into the cell together with the sample. From the linear frequency shift of the R_1-fluorescence line of ruby (−7.6 cm^{-1}/GPa).[30] we have determined the pressure in the cell to be $\Delta p = 3.6$ GPa (36 kbar). This corresponds to a shift of the ruby fluorescence line of 27.9 cm^{-1}.

The experiments at ambient ($\Delta p = 0$) and high pressure ($\Delta p = 3.6$ GPa) were carried out in a ^{4}He-bath cryostat between 1.2 and 4.2 K. At $\Delta p = 0$, the sample was placed either in a 1 mm flat cuvette or frozen on a glass plate and then quickly introduced into the cryostat filled with liquid N_2. After a few minutes, the liquid N_2 was blown out and the cryostat filled with liquid helium. For high pressure experiments, the diamond-anvil cell containing the sample was placed in the cryostat. The latter was then filled with liquid N_2 and the same cooling procedure was followed as above. The temperature in the cryostat was determined by means of a calibrated carbon resistor close to the sample using a 4-point method and, simultaneously, by the vapor pressure of the helium, with an accuracy of ±0.005 K.[21]

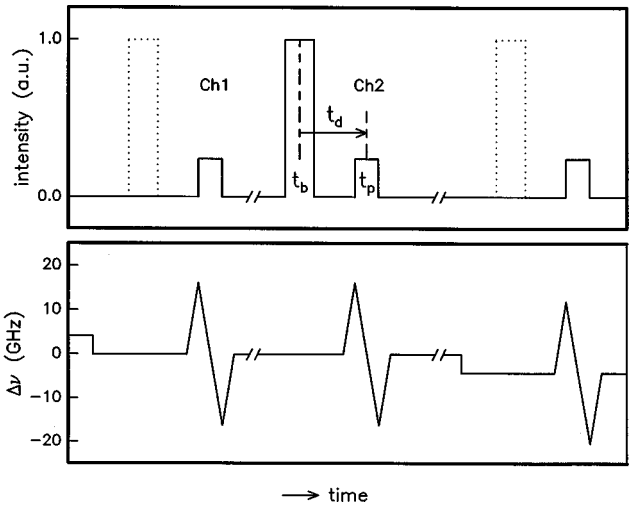

FIG. 1. Pulse sequence used in time-resolved hole-burning. Top: timing of the laser pulses. Bottom: frequency-ramp and frequency-steps. t_b: burn time, t_d: delay time, t_p: probe time, $\Delta\nu$: change in laser frequency.

B. Experimental setup

Absorption spectra were measured with a cw Titanium: sapphire ring laser (Coherent 899-21, *without* intracavity etalon, linewidth $\Gamma_{laser} \approx 6$ GHz), pumped by an Ar^+ laser. The wavelength of the laser was calibrated with a home-built Michelson interferometer (frequency≈50 MHz).

The pulse sequence used to burn and probe holes is shown in Fig. 1. It consists of three steps: first, a base line is measured at low laser intensity. During this time the frequency of the laser is scanned over the part of the inhomogeneous absorption band in which a hole will be burnt. Then, a hole is burnt at a fixed frequency during a time t_b at higher intensity than that used for the base line (factor $10-10^3$) during a time t_b. Finally, after a variable delay time t_d, the hole is probed for a time t_p. During the time t_p, the frequency of the laser is scanned again (at low intensity) over the region of the hole. To obtain the hole profile, the difference between the signals before and after burning is recorded.[6]

To perform time-resolved hole-burning experiments we used two types of cw single-frequency lasers. The choice of the laser depends on the time scale of the experiment. For short delay times between microseconds and a few seconds, we use three current-controlled (Seastar, LD 2000, $\Delta I/I \approx 4\times10^{-6}$, modulation bandwidth 2 MHz) and temperature-controlled (ILX Lightwave, LDT 5910, stability better than 0.01 °C) single-mode diode lasers: Hitachi HL 7806G. HL 8325G, and Sharp LT030-MD emitting at different wavelengths. The main advantage of semiconductor lasers is that

their frequency can be scanned very fast (up to ~10 GHz/μs) by sweeping the current through the diode.[6,31] A disadvantage is their restricted tunable wavelength region (5 to 10 nm by changing the laser temperature). The bandwidth of these diode lasers is ~6 MHz for the HL 8325G (tuning range 818–828 nm), ~50 MHz for the HL 7806G (780–793 nm), and ~60 MHz for the LT030-MD (751–760 nm).[31]

For delay times longer than ~100 ms, we used the cw single-frequency Titanium:sapphire ring laser, but now *with* an intracavity etalon (Coherent 899-21, bandwidth ~0.5 MHz, tunable from ~700 to 1000 nm, amplitude stabilized to better than 0.5%). The frequency of this laser can be scanned continuously over 30 GHz with a maximum scan speed of ~100 MHz/ms. This speed is about 100 000 times slower than that of the diode lasers.

The wavelength of all the lasers was calibrated with the Michelson interferometer, and their mode structure was monitored with a confocal Fabry–Perot (FP) etalon (FSR=300 MHz and/or 1.5 GHz).

Burning power-densities between 1 μW/cm^2 and 1 mW/cm^2 were usually used together with burning times from $t_b=1$ μs to ~100 s. The same laser was used for probing, but with its power attenuated by a factor of 10 to 10^3 with respect to burning. The delay time t_d between burning and probing the holes varied from 1 μs to 24 h. Because of the design of the pressure cell, the holes had to be probed in transmission through the sample. The holes were detected with a photomultiplier (EMI 9658R) and the signal was subsequently amplified and averaged, as described in Ref. 23. The experiments were controlled with a personal computer (PC).

C. Determination of the effective homogeneous linewidth Γ'_{hom}

The ''effective'' homogeneous linewidth Γ'_{hom} is determined in the following way: holes are burnt with a given set of parameters (temperature, delay time, wavelength, and pressure) and measured as a function of burning-fluence density Pt_b/A (where P is the burning power of the laser, t_b the burning time, and A the area of the laser spot on the sample). The holewidths are then extrapolated to $Pt_b/A\rightarrow 0$ to take into account the effect of power broadening. This yields a value $\Gamma_{\mathrm{hole},0}(t_b,t_d)$ which is given by:[21]

$$\Gamma_{\mathrm{hole},0}(t_b,t_d)=\Gamma'_{\mathrm{hom}}(t_b)\otimes\Gamma_{\mathrm{laser}}\otimes\Gamma'_{\mathrm{hom}}(t_d)\otimes\Gamma_{\mathrm{laser}}, \quad (2.1)$$

where $\otimes$ represents a convolution, $\Gamma'_{\mathrm{hom}}(t_i)$ is what we call the effective homogeneous linewidth at time t_i, and Γ_{laser} is the bandwidth of the laser (varying from 0.5 MHz for the Titanium:sapphire laser, to ~60 MHz for the LT030MD/MF diode lasers).[31] Because the holes are generally well fitted with Lorentzian curves, the convolution in Eq. (2.1) becomes a sum. To determine $\Gamma'_{\mathrm{hom}}(t_d)$, the quantity of interest, a hole-burning experiment is first performed at delay time $t_d=t_b$,

$$\Gamma_{\mathrm{hole},0}(t_b,t_d)=2\Gamma'_{\mathrm{hom}}(t_b)+2\Gamma_{\mathrm{laser}}. \quad (2.2)$$

Inserting $\Gamma'_{\mathrm{hom}}(t_b)$ from Eq. (2.2) into the sum corresponding to Eq. (2.1) yields:

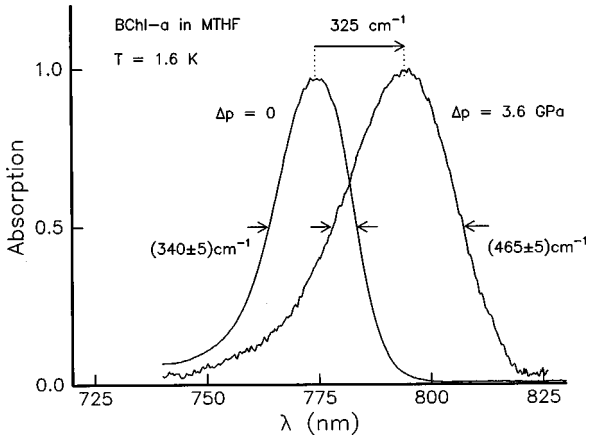

FIG. 2. Absorption spectrum of the $S_1\leftarrow S_0$ 0–0 band (Q_y-region) of BChl-a in MTHF at ambient pressure ($\Delta p=0$) and high pressure ($\Delta p=3.6$ GPa), at $T=1.6$ K. Under pressure, the band shifts to the red from 775 nm to 795 nm, and broadens from 340 cm^{-1} to 465 cm^{-1}.

$$\Gamma'_{\mathrm{hom}}(t_d)=\Gamma_{\mathrm{hole},0}(t_b,t_d)-(1/2)\Gamma_{\mathrm{hole},0}(t_b,t_b)-\Gamma_{\mathrm{laser}}. \quad (2.3)$$

For $t_d\leqslant 100$ s, we used $t_b=t_d$. Equation (2.3) then reduces to

$$\Gamma'_{\mathrm{hom}}(t_d)=(1/2)\Gamma_{\mathrm{hole},0}(t_b,t_b)-\Gamma_{\mathrm{laser}}. \quad (2.4)$$

Whenever $t_d>t_b$, Eq. (2.3) has to be used. Notice that for $t_d\gg t_b$:

$$\Gamma'_{\mathrm{hom}}(t_d)\approx\Gamma_{\mathrm{hole},0}(t_b,t_d)-2\Gamma_{\mathrm{laser}}. \quad (2.5)$$

III. RESULTS AND DISCUSSION

A. Absorption spectra

Figure 2 shows the effect of pressure on the $S_1\leftarrow S_0$ 0–0 transition (Q_y-band) of BChl-a in MTHF at $c=5\times10^{-4}$ and $T=1.6$ K. For $\Delta p=3.6$ GPa, the maximum of the band shifts to the red from 773 to 790 nm, which corresponds to -90 cm^{-1}/GPa. This value is comparable to those reported in the literature for organic glassy systems[21,32–37] and photosynthetic proteins.[38] The shift is caused by an increase of the polarizability of the host material under pressure because of its higher density. This, in turn, leads to an increase of the solvent shift,[39] which usually is linear in pressure. We have also observed a broadening of the Q_y-band of ~35 cm^{-1}/GPa (Fig. 2). Such a broadening, also observed for rhodamine 101 in PMMA[35] and photosynthetic pigment-protein complexes,[38] is due to the lifting of the accidental degeneracy of the energy levels. This is in contrast to the narrowing of the Q_y-band observed for BChl-a in triethylamine (TEA) under high pressure.[21] The latter was attributed to a structural transition taking place in TEA from a glass at $\Delta p=0$ to a crystal at high pressure.[21]

B. Optical dephasing: Γ'_{hom} vs. T

Figure 3 shows that the effective homogeneous linewidth Γ'_{hom} follows a $T^{1.3\pm0.1}$ temperature dependence between 1.2 and 4.2 K when holes are burnt in the *red wing* of the absorption band (790 nm, open symbols). Such a depen-

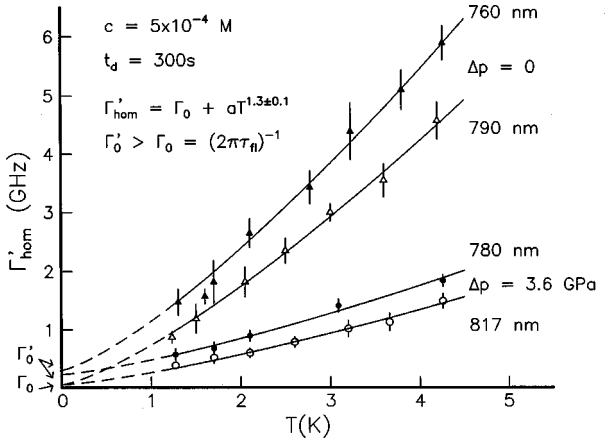

FIG. 3. Temperature dependence of the effective homogeneous linewidth $\Gamma'_{\rm hom}$ of the 0–0 band of BChl-*a* in MTHF at $c=5\times10^{-4}$ M, in the red wing (open symbols) and blue wing (closed symbols), for $\Delta p=0$ (upper curves), and $\Delta p=3.6$ GPa (lower curves). All data follow a $T^{1.3\pm0.1}$ power law. In the red wing, $\Gamma'_{\rm hom}$ extrapolates to $\Gamma_0=(2\pi\tau_{\rm fl})^{-1}$ for $T\rightarrow0$; in the blue wing, it extrapolates to $\Gamma'_0>\Gamma_0$ due to extra spectral diffusion induced by energy transfer.

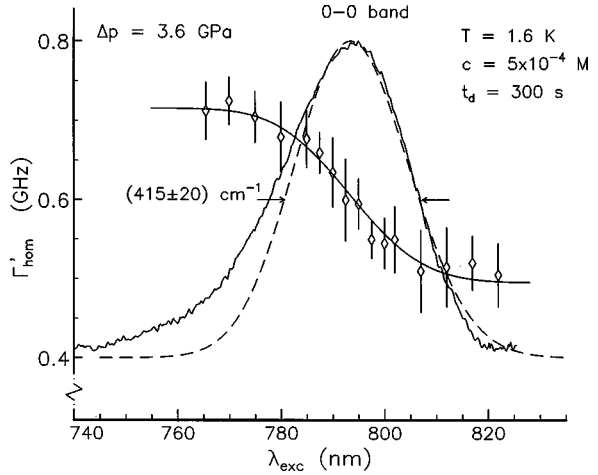

FIG. 4. Dependence of $\Gamma'_{\rm hom}$ on excitation wavelength $\lambda_{\rm exc}$ at $\Delta p=3.6$ GPa, $T=1.6$ K and $t_d=300$ s. $\Gamma'_{\rm hom}$ increases towards the blue following an *S*-shaped curve which represents the integral of a Gaussian (dashed curve) to the red of $\lambda_{\rm exc}$. It is proportional to the number of BChl-*a* molecules absorbing at wavelengths longer than $\lambda_{\rm exc}$.

dence is characteristic for organic glasses[13,16,17] and is determined by the presence of TLSs. Under high pressure ($\Delta p=3.6$ GPa), the red wing of the absorption band shifts to the red (817 nm) and the value of $\Gamma'_{\rm hom}$ decreases significantly. However, the $T^{1.3\pm0.1}$ power law remains, implying that MTHF is still a ''true'' glass. In contrast, materials like TEA,[21] methanol,[24] and ethanol[25] become crystalline under pressure. Both curves in Fig. 3, at $\Delta p=0$ and $\Delta p=3.6$ GPa, extrapolate to $\Gamma_0=(2\pi\tau_{\rm fl})^{-1}$ for $T\rightarrow0$, with $\tau_{\rm fl}=4$ ns for BChl-*a*.

In the *blue wing* (Fig. 3), $\Gamma'_{\rm hom}$ again follows a $T^{1.3\pm0.1}$ power law at ambient (760 nm) and high pressure (780 nm), but extrapolates to $\Gamma'_0>\Gamma_0$. The mechanism responsible for the larger residual linewidth, as is shown below (Sec. III C to E), is energy-transfer-induced spectral diffusion, ET→SD.[21–23] We would, therefore, expect that $\Gamma'_{\rm hom}$ not only depends on excitation wavelength $\lambda_{\rm exc}$, but also on delay time t_d between burning and probing the hole, even at $T\rightarrow0$.[22]

C. Indirect effect of energy transfer: $\Gamma'_{\rm hom}$ vs. $\lambda_{\rm exc}$

The dependence of $\Gamma'_{\rm hom}$ on excitation wavelength $\lambda_{\rm exc}$ at $\Delta p=3.6$ GPa is shown in Fig. 4, superimposed on the 0–0 absorption band. The data follow an *S*-shaped curve which represents the integral of the dashed Gaussian curve. Thus, each point on the *S*-shaped curve is proportional to the number of molecules absorbing to the red of the excitation wavelength. Because the Gaussian is centered in the middle of the 0–0 absorption band, we conclude that all BChl-*a* molecules (or a wavelength-independent fraction of them) are active in a process that is not direct ET, but triggered by downhill energy transfer. This ET→SD effect is typical for glasses.[20–23] The idea is the following: during the excited-state lifetime of $\tau_{\rm fl}=4$ ns of BChl-*a*, excitation energy is transferred stepwise and downhill from one excited probe molecule to another absorbing further to the red. At each step, part of the mismatch of the excitation energy of donor and acceptor molecules ΔE is released as ''heat'' into the MTHF glass. By this mechanism, a large part of the glass in the vicinity of the BChl-*a* molecules is explored during their lifetime of 4 ns in the excited state, and energy can be stored in TLSs. These ''activated'' TLSs, which give rise to ''extra'' SD, will relax back to equilibrium on a very long time scale. Thus, $\Gamma'_{\rm hom}$ increases with delay time, even at $T\rightarrow0$, and towards the blue within the 0–0 absorption band. Since this extra SD is induced by ET, this effect was called ET→SD.[20,22] We attribute the small discrepancy between the dashed Gaussian and the 0–0 band in the blue wing to vibronic bands in the absorption spectrum. It is noteworthy that the Gaussian previously derived from the *S*-shaped curve in TEA doped with BChl-*a* did not coincide with the maximum of the 0–0 absorption band, like in MTHF, but was blue-shifted by ~135 cm^{-1} at $\Delta p=0$ and by ~70 cm^{-1} at $\Delta p=3.6$ GPa.[21] An interpretation was given in terms of TLSs with barrier heights of ~100 cm^{-1} characteristic of TEA. These barriers first have to be crossed before spectral diffusion occurs.

D. Spectral diffusion: $\Gamma'_{\rm hom}$ vs. t_d

The dependence of $\Gamma'_{\rm hom}$ on temperature at two delay times, $t_d=20\,\mu$s and 300 s, is shown in Fig. 5, for $\Delta p=3.6$ GPa in the blue and red wings of the absorption band. The value of $\Gamma'_{\rm hom}$ increases with delay time proving that there is spectral diffusion. In the red (817 nm), both curves, for short and long delay times, extrapolate to the fluorescence lifetime-limited value $\Gamma_0=(2\pi\tau_{\rm fl})^{-1}$ for $T\rightarrow0$, because of the absence of downhill ET. In the blue wing, however, $\Gamma'_0>\Gamma_0$. Furthermore, we see that Γ'_0 not only depends on excitation wavelength and the amount of pressure applied, but also on delay time t_d. The values of Γ'_0 and *a*, obtained from the data, are given in Table I for $\Delta p=0$ and $\Delta p=3.6$ GPa. The interpretation of the results is discussed in Sec. III E.

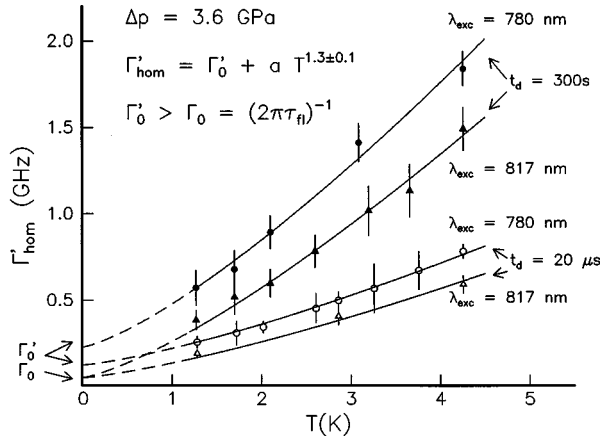

FIG. 5. Γ'_{hom} as a function of temperature at $\Delta p = 3.6$ GPa for two delay times, $t_d = 15\ \mu$s and 300 s, in the blue (780 nm) and red (817 nm) wings of the 0–0 band. Γ'_{hom} increases with delay time, implying that there is spectral diffusion (SD). In the red wing, Γ'_{hom} extrapolates to Γ_0 for $T \to 0$; in the blue wing, to $\Gamma'_0(t_d) > \Gamma_0$. Since Γ'_0 also increases with delay time, extra SD is triggered by downhill energy transfer, in addition to normal SD.

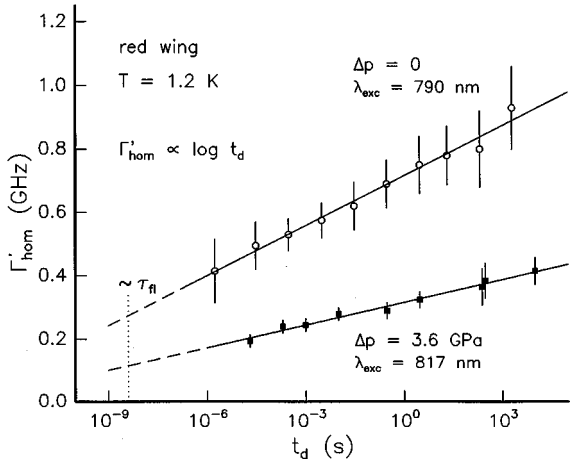

FIG. 6. Γ'_{hom} as a function of the logarithm of the delay time, at $\Delta p = 0$ and 3.6 GPa, in the red wing of the 0–0 band (absence of ET), at $T = 1.2$ K. Γ'_{hom} is linearly proportional to $\log t_d$. The amount of normal SD, defined as $d\Gamma'_{\mathrm{hom}}/d(\log t_d)$, decreases under pressure.

In Fig. 6, the results for Γ'_{hom} in the *red wing* have been plotted as a function of the logarithm of the delay time, for $\Delta p = 0$ and $\Delta p = 3.6$ GPa. In the red wing, the influence of downhill energy transfer can be neglected. The two curves follow a linear dependence on $\log t_d$, which is consistent with a hyperbolic distribution of relaxation rates $P(R) = 1/R$ within the TLS model of glasses.[5] We assign the slope $d\Gamma'_{\mathrm{hom}}/d \log t_d$ to normal spectral diffusion (SD) not affected by energy transfer; this slope is lower at $\Delta p = 3.6$ GPa than at $\Delta p = 0$ by about 60%. We attribute this decrease to the reduction of free volume in the glass under pressure and, therefore, to a decrease in the number (or density) of TLSs.

The effect of excitation wavelength, i.e., of indirect downhill ET, on the amount of SD under high pressure is given in Fig. 7. Γ'_{hom} versus $\log t_d$ at $T = 1.2$ K is plotted for three values of λ_{exc}, from the red to the blue wing. Again, the dependence of Γ'_{hom} on $\log t_d$ is linear, but the amount of SD increases to the blue, implying that extra SD, in addition to normal SD, is induced by downhill energy transfer. The amount of spectral diffusion increases proportionally to $T^{1.3\pm0.1}$ between 1.2 and 4.2 K, for $\Delta p = 0$ and $\Delta p = 3.6$ GPa (results not shown), proving that a larger number of TLSs is active at higher temperatures. As a consequence, also the amount of SD increases.

TABLE I. The residual linewidth Γ'_0 and the coupling constant a at the blue and red wing of the $S_1 \leftarrow S_0$ 0–0 absorption band of BChl-*a* in MTHF, for two delay times, at $\Delta p = 0$ and $\Delta p = 3.6$ GPa.

λ_{exc}	t_d (s)	Γ'_0 (MHz)	a (MHz/K$^{1.3}$)
$\Delta p = 0$			
790 nm (red wing)	1.5×10^{-5}	50	0.31
	3×10^{2}	50	0.69
760 nm (blue wing)	1.5×10^{-5}	140	0.34
	3×10^{2}	300	0.85
$\Delta p = 3.6$ GPa			
817 nm (red wing)	1.5×10^{-5}	50	0.09
	3×10^{2}	50	0.21
780 nm (blue wing)	1.5×10^{-5}	120	0.10
	3×10^{2}	226	0.25

E. Residual linewidth and coupling constant

The results of Figs. 3 to 7 can now be combined to construct Figs. 8(a),(b). The delay time dependence of Γ'_0 is depicted in Fig. 8(a). Notice that in the expression:

$$\Gamma'_0 = \Gamma_0 + \Gamma_0^{\mathrm{ET}}(\lambda_{\mathrm{exc}} c) + \Gamma_0^{\mathrm{ET}\to\mathrm{SD}}(\lambda_{\mathrm{exc}}, c, t_d), \tag{3.1}$$

where $\Gamma_0 = (2\pi\tau_{\mathrm{fl}})^{-1}$ is the fluorescence lifetime-limited value and Γ_0^{ET} is the downhill energy transfer rate, only $\Gamma_0^{\mathrm{ET}\to\mathrm{SD}}$ depends on delay time. This term contributes with extra SD to Γ'_0 due to downhill ET. In the red wing, at $\Delta p = 0$ and $\Delta p = 3.6$ GPa, $\Gamma'_0 = \Gamma_0$ because of the absence of downhill ET [the horizontal line in Fig. 8(a)]. In the blue wing, the slope $d\Gamma'_{\mathrm{hom}}/d \log t_d$ is larger for $\Delta p = 0$ than for $\Delta p = 3.6$ GPa. By extrapolating the data to $t_d = \tau_{\mathrm{fl}}$, we may

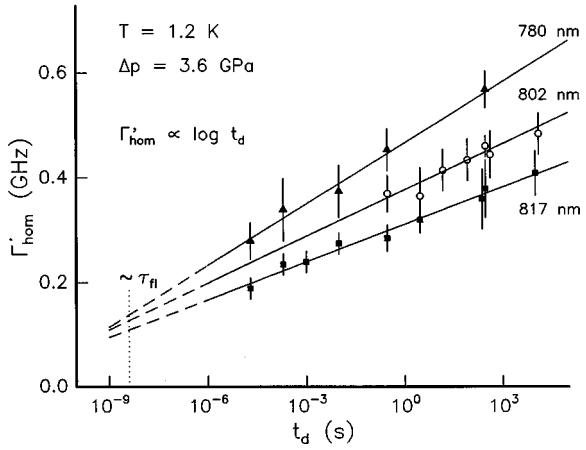

FIG. 7. Dependence of Γ'_{hom} on $\log t_d$ at $\Delta p = 3.6$ GPa, for three excitation wavelengths $\lambda_{\mathrm{exc}} = 780$, 802, and 817 nm. The amount of extra SD, $d\Gamma'_{\mathrm{hom}}/d(\log t_d)$, increases towards the blue wing of the 0–0 band due to downhill ET.

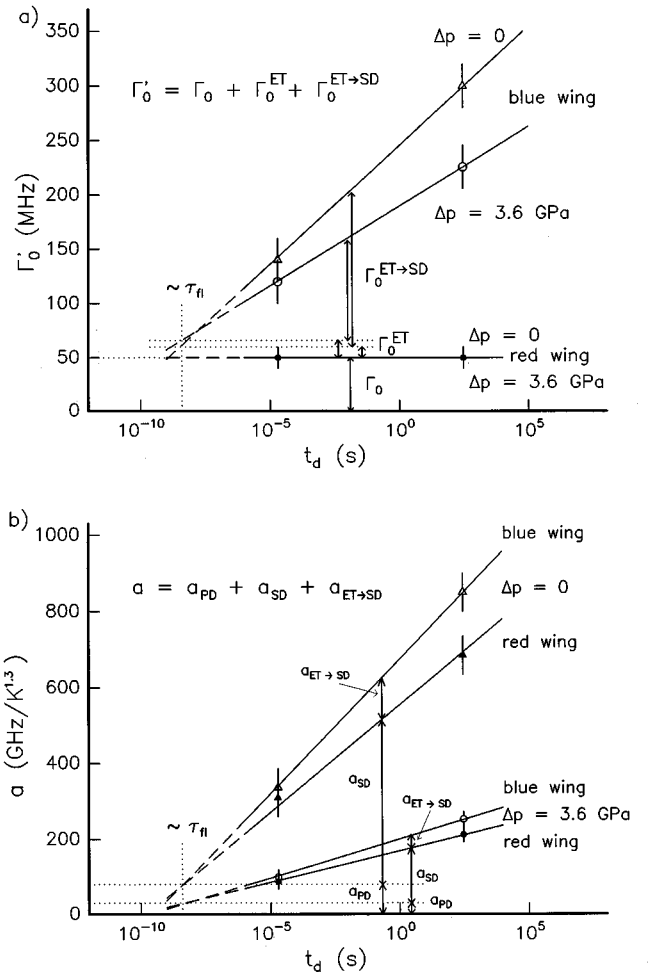

FIG. 8. (a) Dependence of the residual linewidth Γ_0' on $\log t_d$ in the blue wing (upper curves) and red wing (lower curves) of the 0–0 band, for $\Delta p = 0$ and $\Delta p = 3.6$ GPa. In the red wing, $\Gamma_0' = \Gamma_0 = (2\pi\tau_{fl})^{-1}$. In the blue wing, values for the higher limit of the energy-transfer rate Γ_0^{ET} are obtained by extrapolating Γ_0' to $t_d \approx \tau_{fl} \approx 4$ ns. At any given $t_d > \tau_{fl}$, $\Gamma_0' = \Gamma_0 + \Gamma_0^{ET} + \Gamma_0^{ET\to SD}$. (b) Coupling constant a as a function of $\log t_d$ in the blue and red wings of the 0–0 band at ambient (upper curves) and high pressure (lower curves). By extrapolating a to $t_d \approx \tau_{fl} \approx 4$ ns one obtains the value of a_{PD}. At any given $t_d > \tau_{fl}$, $a = a_{PD} + a_{SD}(t_d)$ in the red wing. Towards the blue, there is an additional contribution $a_{ET\to SD}(t_d)$ due to extra SD induced by downhill energy transfer.

estimate the values for Γ_0^{ET}, since downhill energy transfer takes place within the lifetime of the excited state. We obtain $\Gamma_0^{ET} \approx (10 \pm 5)$ MHz at ambient pressure, and $\Gamma_0^{ET} \approx (16 \pm 5)$ MHz at high pressure.

The difference between the values of Γ_0^{ET} at $\Delta p = 0$ and $\Delta p = 3.6$ GPa can be explained as follows. If we assume an energy transfer mechanism of the Förster-type, i.e., a dipole–dipole interaction between the BChl-*a* molecules, the rate Γ_0^{ET} is proportional to $1/r^6$, where r is the distance between the donor and acceptor molecules, and, therefore, to $1/V^2$, where V is the volume. The volume reduction under pressure can be calculated using Murnaghan's equation:[21,40]

$$\Delta p = B_T/B_T' \, [(V_0/V_{\Delta p})^{B_T'} - 1], \tag{3.2}$$

with B_T the zero-pressure bulk modulus, B_T' the derivative of B_T with respect to pressure, $V_{\Delta p}$ the volume at high pressure, and V_0 the volume at ambient pressure. By using the same empirical constants for $B_T \sim 5-7$ GPa and $B_T' \sim 7-8$, as previously used in,[21] we obtain for $\Delta p = 3.6$ GPa:

$$V_{\Delta p}/V_0 = 0.80, \tag{3.3}$$

i.e., a volume decrease of 20%. The value of Γ_0^{ET} is thus expected to increase with pressure proportionally to $(V_0/V_{\Delta p})^2 = 1/(0.8)^2 = 1.6$. This increase is in agreement with the estimated values of Γ_0^{ET} at $\Delta p = 0$ and $\Delta p = 3.6$ GPa in Fig. 8(a):

$$\frac{(\Gamma_0^{ET})_{\Delta p = 3.6\ \mathrm{GPa}}}{(\Gamma_0^{ET})_{\Delta p = 0}} \approx \frac{16\ \mathrm{MHz}}{10\ \mathrm{MHz}} = 1.6. \tag{3.4}$$

We attribute the difference between the measured value Γ_0' and $(\Gamma_0 + \Gamma_0^{ET})$ to $\Gamma_0^{ET\to SD}$. The latter should extrapolate to zero at $t_d = \tau_{fl}$, because SD only takes place after the molecules have decayed back to the ground state. We see in Fig. 8(a) that the amount of extra SD induced by ET is larger at $\Delta p = 0$ than at $\Delta p = 3.6$ GPa. It is surprising that although the energy transfer rate Γ_0^{ET} is larger under pressure and downhill ET triggers extra SD, $\Gamma_0^{ET\to SD}$ decreases under pressure. The explanation for this effect is that the number of TLSs actively participating in SD is reduced under pressure. Apparently, the effect of high pressure is predominantly through a reduction of the free volume rather than through an increase of the value of Γ_0^{ET} due to a decrease of the intermolecular distances between BChl-*a* molecules. The net effect is a significant decrease in the amount of spectral diffusion.

In Figure 8(b) the coupling constant

$$a = a_{PD} + a_{SD}(t_d) + a_{ET\to SD}(t_d), \tag{3.5}$$

is plotted versus the logarithm of delay time t_d. In Eq. (3.5), a_{PD} is the ''pure'' dephasing term, a_{SD} the ''normal'' spectral diffusion term, and $a_{ET\to SD}$ is the contribution of energy-transfer-induced spectral diffusion to the coupling constant.[23] As for Γ_0', we observe a significant decrease of a under high pressure due to the reduction of the number (or density) of active TLSs. By extrapolating the curves to $t_d = \tau_{fl}$, we obtain the value of a_{PD}. At $t_d < \tau_{fl}$, both normal and extra SD are absent. At delay times $t_d > \tau_{fl}$ and in the red wing, the only contributions to a come from a_{PD} and a_{SD}, whereas in the blue wing there is also extra SD due to ET. Note in Fig. 8(a),(b) that $\Gamma_0^{ET\to SD}$ and $a_{ET\to SD}$ are proportional to $\log t_d$.[23] This indicates that, within experimental error, the activated TLSs have not relaxed to thermal equilibrium over the time scale of the experiment. The values obtained for a_{PD}, a_{SD}, and $a_{ET\to SD}$ are listed in Table II. They decrease at high pressure due to the reduction of free volume which appears to be correlated with the number of active TLSs.

IV. CONCLUSIONS

In this study we have shown that the dynamics of glasses and, in particular, spectral diffusion (SD) can strongly be influenced by high pressure. We have determined the temperature-, delay time-, and excitation-wavelength-dependence of the ''effective'' homogeneous linewidth Γ_{hom}' of the $S_1 \leftarrow S_0$ 0–0 transition of BChl-*a* in the glass MTHF,

TABLE II. The six contributions to the residual linewidth Γ_0' and to the coupling constant a. They arise from the fluorescence decay rate $\Gamma_0 = (2\pi\tau_{fl})^{-1}$, the downhill energy transfer rate Γ_0^{ET}, pure dephasing a_{PD}, normal spectral diffusion a_{SD}, and two contributions from extra spectral diffusion induced by energy transfer $\Gamma_0^{ET\to SD}$ and $a_{ET\to SD}$, under various conditions.

	$t_d = 1.5\times10^{-5}$ s	$t_d = 3\times10^{2}$ s
$\Delta p = 0$		
Γ_0 (MHz)	50	50
Γ_0^{ET} (MHz)	10	10
$\Gamma_0^{ET\to SD}$ (MHz)	82	240
a_{PD} (MHz/K$^{1.3}$)	80	80
a_{SD} (MHz/K$^{1.3}$)	210	610
$a_{ET\to SD}$ (MHz/K$^{1.3}$)	51	160
$\Delta p = 3.6$ GPa		
Γ_0 (MHz)	50	50
Γ_0^{ET} (MHz)	16	16
$\Gamma_0^{ET\to SD}$ (MHz)	54	160
a_{PD} (MHz/K$^{1.3}$)	30	30
a_{SD} (MHz/K$^{1.3}$)	60	180
$a_{ET\to SD}$ (MHz/K$^{1.3}$)	14	40

at ambient ($\Delta p = 0$) and high ($\Delta p = 3.6$ GPa) pressure. We attribute the decrease of Γ_{hom}' and of $d\Gamma_{hom}'/d\log t_d$ with pressure to a reduction of the free volume in the glass and, consequently, to the number of TLSs active in SD (or, equivalently, to an increase of the TLSs' barrier heights). In the red wing, i.e., in the absence of energy transfer, the reduction of the number of TLSs yields a decrease of normal SD. In the blue wing, at a concentration of $c = 5\times10^{-4}$, downhill energy transfer ET takes place. Apparently, the increase of energy transfer that triggers extra SD is not large enough to compensate for the decrease in the number of active TLSs. We conclude that high pressure not only decreases the amount of normal SD, but also that of extra SD due to ET→SD.

ACKNOWLEDGMENTS

We thank J. H. van der Waals and R. J. Silbey for their comments on the manuscript. The investigations were financially supported by the Netherlands Foundation for Physical Research (FOM) and the Council for Chemical Sciences of the Netherlands Organization for Scientific Research (CW-NWO).

[1] K. A. Littau, M. A. Dugan, S. Chen, and M. D. Fayer, J. Chem. Phys. **96**, 3484 (1992), and references therein.
[2] (a) H. C. Meijers and D. A. Wiersma, Phys. Rev. Lett. **68**, 381 (1992); (b) **101**, 6927 (1994).
[3] Y. S. Bai and M. D. Fayer, Chem. Phys. **128**, 135 (1988); Phys. Rev. B **39**, 11066 (1989).
[4] A. Suarez and R. J. Silbey, Chem. Phys. Lett. **218**, 495 (1994).
[5] R. J. Silbey, J. M. A. Koedijk, and S. Völker, J. Chem. Phys. **105**, 901 (1996).
[6] J. M. A. Koedijk, R. Wannemacher, R. J. Silbey, and S. Völker, J. Phys. Chem. **100**, 19945 (1996).
[7] P. W. Anderson, B. I. Halperin, and C. M. Varma, Philos. Mag. **25**, 1 (1972); W. A. Phillips, J. Low Temp. Phys. **7**, 351 (1972).
[8] *Amorphous Solids: Low Temperature Properties*, edited by W. A. Philips (Springer, Berlin, 1981); W. A. Phillips, Rep. Prog. Phys. **50**, 1657 (1987).
[9] R. Maynard, R. Rammal, and R. Suchail, J. Phys. (France) Lett. **41**, L-291 (1980).
[10] J. L. Black and B. I. Halperin, Phys. Rev. B **16**, 2879 (1977).
[11] P. Hu and L. R. Walker, Solid State Commun. **24**, 813 (1977); Phys. Rev. B **18**, 1300 (1978).
[12] M. H. Cohen and G. S. Grest, Phys. Rev. Lett. **45**, 1271 (1980); Solid State Commun. **39**, 143 (1981).
[13] S. Völker, in *Relaxation Processes in Molecular Excited States*, edited by J. Fünfschilling (Kluwer, Dordrecht, 1985), pp. 113–242, and references therein; Annu. Rev. Phys. Chem. **40**, 499 (1989), and references therein.
[14] J. Lumin. **36**, 179 (1987), and references therein.
[15] R. Wannemacher, J. M. A. Koedijk, R. J. Silbey, and S. Völker, Chem. Phys. Lett. **206**, 19 (1993).
[16] H. P. H. Thijssen, A. I. M. Dicker, and S. Völker, Chem. Phys. Lett. **92**, 7 (1982); H. P. H. Thijssen, R. van den Berg and S. Völker, *ibid.* **97**, 295 (1983).
[17] R. van den Berg, A. Visser, and S. Völker, Chem. Phys. Lett. **144**, 105 (1988).
[18] Th. Schmidt, J. Baak, D. A. van de Straat, H. B. Brom, and S. Völker, Phys. Rev. Lett. **70**, 3584 (1993).
[19] D. L. Huber, J. Lumin, J. Lumin. **36**, 307 (1987); W. O. Puttika and D. L. Huber, Phys. Rev. B **36**, 3436 (1987).
[20] F. T. H. den Hartog, M. P. Bakker, J. M. A. Koedijk, T. M. H. Creemers, and S. Völker, J. Lumin. **66&67**, 1 (1996).
[21] T. M. H. Creemers, J. M. A. Koedijk, I. Y. Chan, R. J. Silbey, and S. Völker, J. Chem. Phys. **107**, 4797 (1997).
[22] F. T. H. den Hartog, M. P. Bakker, R. J. Silbey, and S. Völker, Chem. Phys. Lett. **297**, 314 (1998).
[23] F. T. H. den Hartog, C. van Papendrecht, R. J. Silbey, and S. Völker, J. Chem. Phys. **110**, 1010 (1999).
[24] M. J. P. Brugmans and W. L. Vos, J. Chem. Phys. **103**, 2661 (1995).
[25] J. F. Mammone, S. K. Sharma, and M. Nicol, J. Phys. Chem. **84**, 3130 (1980); A. Anderson and W. Smith, Chem. Phys. Lett. **257**, 143 (1996).
[26] H. van der Laan, H. E. Smorenburg, Th. Schmidt, and S. Völker, J. Opt. Soc. Am. B **9**, 931 (1992).
[27] K. Iriyama, N. Ogura, and A. Takamiya, J. Biol. Chem. **76**, 901 (1974); K. Iriyama, M. Yoshiura, T. Ishii, and M. Shiraki, J. Liq. Chrom **4**, 533 (1981).
[28] L. Merrill and W. A. Bassett, Rev. Sci. Instrum. **45**, 290 (1974).
[29] I. Y. Chan, C. M. Wong, and D. Stehlik, Chem. Phys. Lett. **219**, 187 (1994).
[30] R. A. Forman, G. J. Piermarini, J. D. Barnett, and S. Block, Science **176**, 284 (1972).
[31] U. Störkel, J. M. A. Koedijk, R. Wannemacher, F. T. M. den Hartog, M. P. Bakker, C. van Papendrecht, T. M. M. Creemers, A. J. Lock, and S. Völker (unpublished).
[32] A. Freiberg, A. Ellervee, P. Kukk, A. Laisaar, M. Jars, and K. Timpmen, Chem. Phys. Lett. **214**, 10 (1993).
[33] M. Croci, H. J. Müschenborn, F. Güttler, A. Renn, and U. P. Wild, Chem. Phys. Lett. **212**, 71 (1993), and references therein.
[34] A. Ellervee, J. Kikas, A. Laisaar, V. Shcherbakov, and A. Suisalu, J. Opt. Soc. Am. B **9**, 972 (1992).
[35] A. Müller, R. Richter, and L. Kador, Chem. Phys. Lett. **241**, 547 (1995).
[36] R. A. Crowell and E. L. Chronister, Chem. Phys. Lett. **216**, 293 (1993).
[37] B. J. Baer, R. A. Crowell, and E. L. Chronister, Chem. Phys. Lett. **237**, 380 (1995).
[38] H. C. Chang, R. Jankowiak, N. R. S. Reddy, and G. J. Small, Chem. Phys. **197**, 307 (1995).
[39] Th. Sesselmann, W. Richter, D. Haarer, and H. Morawitz, Phys. Rev. B **36**, 7601 (1987).
[40] J. M. Lang and H. G. Drickamer, J. Phys. Chem. **97**, 5058 (1993).